Efficient Indoor Signal Propagation Model Based on LOLA-Voronoi Adaptive Meshing

Junyi Yao [1], Wanchun Tang [*2, 3], Baozhu Li [1], Shuming Zhang [1], and Rui Sun [1]

[1] School of Physics and Technology
Nanjing Normal University, Nanjing, 210023, China
1016424781@qq.com, 951408095@qq.com, 1627839409@qq.com, 1067311237@qq.com

[2] School of Electrical and Automation Engineering, Nanjing Normal University, Nanjing, 210023, China

[3] Jiangsu Center for Collaborative Innovation in Geographical Information Resource Development and Application
Nanjing, 210023, China
eewctang@njnu.edu.cn

Abstract **─** An innovative adaptive mesh strategy based on LOLA-Voronoi (Local Linear Approximation-Voronoi) is proposed to efficiently predict indoor signal propagation. This indoor high-efficiency propagation model (HPMO) can identify nonlinear regions to capture the complex behavior and achieve sufficient prediction accuracy when the computational cost is limited. A set of representative reference scenario simulation settings and results are reported and discussed to analyze the accuracy, and the efficiency of HPMO. Comparison with the original model based on traditional uniform mesh shows that the proposed method herein yields a considerable reduction in the prediction calculation cost of the complex indoor environment, while maintaining sufficient accuracy.

Index Terms **─** HPMO, indoor signal propagation model, LOLA-Voronoi, received signal strength.

I. INTRODUCTION

With the growing demand for indoor wireless LANs and personal communication networks, it is very important to adequately consider wireless communication in indoor environments. Recently, indoor localization [1-2], wireless communication system design [3], and human exposure assessment [4] have become popular application areas for indoor electromagnetic environments. Therefore, efficient prediction of indoor radio wave propagation becomes a necessary basic step.

A wide range of methods focused on indoor propagation prediction have been proposed. Deterministic models (such as FDTD, UTD, MoM [4-7]) have high accuracy, however, they are time-consuming due to the inherent computational complexity. On the contrary, empirical models (such as ITU-R, Motley-Keenan, Okumura–Hata, COST-231 [8-11]) have the advantage of rapid implementation, but the accuracy is flawed because the environment is simplified. In [12], multipath effect is considered in the model of radio channel, polarized channel model has also been defined within [13]. A modified Motley-Keenan model based on ray-tracing was developed in [14-15], which takes into account both the multipath effect and beam polarization, thus obtaining the trade-off between accuracy and efficiency. Unfortunately, just uniform meshing is considered in this model and with higher operation frequency, smaller cell sizes, and more advanced antenna systems, radio propagation modeling becomes more difficult and challenging.

To reduce the cost, a new zone-based propagation model based on reduced number of measurements to recover the indoor fingerprint database is taken in [16]. And a reconstruction technology based on 2D LOLA-Voronoi (Local Linear Approximation-Voronoi) adaptive meshing method without any prior knowledge on the source antenna is developed in [17].

LOLA-Voronoi used in [17] is an effective integration of a sequential experimental design (SED). Unlike fixed mesh, LOLA-Voronoi could use information gathered from previous data points to determine the position of new data points adaptively [18]. The outcome of LOLA-Voronoi is a representative set of data samples that is more concentrated within those regions in which larger deviations from a local linear approximation have been calculated starting from a small initial set of samples. And its practical application in complex indoor environment remains to be solved.

This paper aims at proposing an indoor high-efficiency propagation prediction method based on LOLA-Voronoi adaptive meshing. The main contributions are presented here: (a) it's the first attempt to implement an adaptive meshing using LOLA-Voronoi in an indoor

Submitted On: December 9, 2019
Accepted On: February 23, 2020
1054-4887 © ACES

signal strength prediction developed by a modified Motley-Keenan model [14]; (b) the overall cost is reduced, while adequate accuracy is obtained in the computed estimation; (c) an indoor environment is selected as a reference scenario, and RMSE values of different indoor propagation models are calculated to verify the feasibility of the proposed model.

This paper is organized as follows. The modified indoor propagation model and formulation of the LOLA-Voronoi adaptive meshing method and the proposed HPMO are described in Section II. Section III describes the numerical simulation settings, prediction results and comparisons. Section IV concludes the paper.

II. HIGH-EFFICIENCY PROPAGATION MODEL IMPLEMENTATION

A. Modified Motley-Keenan model

The path loss of indoor empirical propagation models are generally expressed as follows:

$$L(d)=L(d_0)+20\log(d)+A\,, \tag{1}$$

where $L(d_0)$ is the free-space loss at a reference distance d_0 of 1m. d is the separation distance between transmit antenna (Tx) and receive antenna (Rx), A represents attenuation in signal strength, which tends to be variant in different models.

A modified Motley-Keenan model [9] based on ray tracing is adopted in this work, A in equation (1) is mathematically expressed as:

$$A=20\log(\frac{4\pi}{\lambda})-10\log(\prod\tau_w)-10\log(\prod\Gamma_w)\,, \tag{2}$$

where λ represents the wavelength, τ_k, Γ_k are respectively the transmission and reflection coefficient when the ray encounters obstacle k, which can be calculated by Fresnel coefficients [19].

The algorithm [15] uniformly divides the 2D research domain into a large number of nodes, and obtains the path loss corresponding to each node using the model expressed in equation (2).

More details are added to the received EM signal strength P (in dB), such as transmit power and antenna directivity:

$$P=P_{\mathrm{Tx}}+G_{\mathrm{Tx}}+G_{\mathrm{Rx}}-L(d)\,, \tag{3}$$

where P_{Tx} is the transmit power, G_{Tx} and G_{Rx} are the transmitter (Tx) and receiver (Rx) antenna gains respectively.

B. LOLA-Voronoi Adaptive meshing

Adaptive meshing based on LOLA-Voronoi is aimed at selecting nodes in unexplored regions of the design space and adding nodes in regions which were previously identified to be interesting such as nonlinear regions [18]. These two measures are combined into a hybrid score to calculate each existing node:

$$S(\mathbf{p}_m)=V(\mathbf{p}_m)+\frac{O(\mathbf{p}_m)}{\sum_{m=1}^{M}O(\mathbf{p}_m)}\,, \tag{4}$$

where $\mathbf{p}_m$ [m=1, 2, …, M] represents any one of the existing nodes, $V(\mathbf{p}_m)$ is the size of Voronoi cell where $\mathbf{p}_m$ is located, representing whether or not under-meshed around this point, the last fraction represents the non-linearity behavior at $\mathbf{p}_m$.

More specifically, Voronoi tessellation is an effective methodology to describe sampling density. It is a set of continuous polygons that connect the vertical bisectors of two adjacent line segments as shown in Fig. 1.

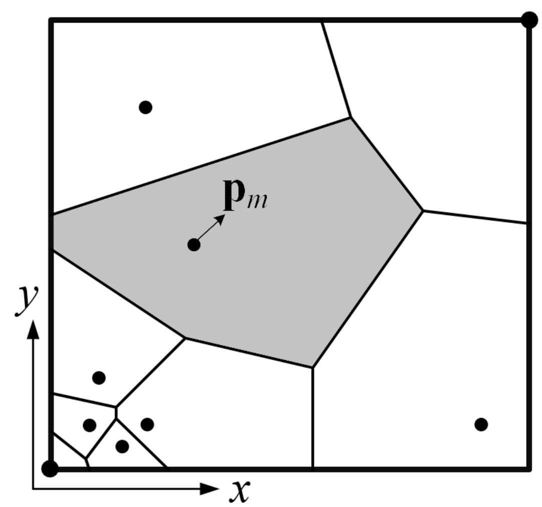

Fig. 1. Voronoi tessellation in design space.

Each cell contains only one node $\mathbf{p}_m$, and the cell size can be approximately estimated as:

$$V(\mathbf{p}_m)=\frac{k}{N}\,, \tag{5}$$

where N is the large number of randomly, evenly distributed Monte Carlo test points [$\mathbf{t}_n$, n=1, 2, …, N] generated in the domain, k denotes the number of test points closest to $\mathbf{p}_m$:

$$\left|\mathbf{t}_n-\mathbf{p}_m\right|\le\left|\mathbf{t}_n-\mathbf{p}_{m'}\right|\,|m\neq m'\,. \tag{6}$$

In addition, the non-linearity can be estimated by the gradient $\mathbf{g}$, which can be calculated by fitting a hyperplane through reference node $\mathbf{p}_m$ and its ith neighbor $\mathbf{p}_{mi}=(\mathbf{p}_{mi}^{(x)},\mathbf{p}_{mi}^{(y)})$ [i=1, 2, …, 4], the following system is solved by least squares:

$$\begin{pmatrix} \mathbf{p}_{m1}^{(x)}-\mathbf{p}_m^{(x)} & \mathbf{p}_{m1}^{(y)}-\mathbf{p}_m^{(y)} \\ \mathbf{p}_{m2}^{(x)}-\mathbf{p}_m^{(x)} & \mathbf{p}_{m2}^{(y)}-\mathbf{p}_m^{(y)} \\ \mathbf{p}_{m3}^{(x)}-\mathbf{p}_m^{(x)} & \mathbf{p}_{m3}^{(y)}-\mathbf{p}_m^{(y)} \\ \mathbf{p}_{m4}^{(x)}-\mathbf{p}_m^{(x)} & \mathbf{p}_{m4}^{(y)}-\mathbf{p}_m^{(y)} \end{pmatrix} \begin{pmatrix} \mathbf{g}_m^{(x)} \\ \mathbf{g}_m^{(y)} \end{pmatrix} = \begin{pmatrix} P(\mathbf{p}_{m1}) \\ P(\mathbf{p}_{m2}) \\ P(\mathbf{p}_{m3}) \\ P(\mathbf{p}_{m4}) \end{pmatrix}, \tag{7}$$

where $P(\mathbf{p}_{mi})$ is the output value (here specifically refers to the received signal strength) corresponding to $\mathbf{p}_{mi}$, $\mathbf{g}=(\mathbf{g}_m^{(x)},\mathbf{g}_m^{(y)})$ is the gradient that is being calculated.

Then, the nonlinearity of the system near $\mathbf{p}_m$ can be obtained by differences between the responses of the neighbors and the local linear approximation, using the following formula:

$$O(\mathbf{p}_m)=\sum_{i=1}^{4}\left|P(\mathbf{p}_{mi})-(P(\mathbf{p}_m)+\mathbf{g}\cdot(\mathbf{p}_{mi}-\mathbf{p}_m))\right|. \quad (8)$$

New node will be selected around the node with higher hybrid score according to equation (4).

C. High-efficiency propagation model based on LOLA-Voronoi

In order to avoid spending considerable amount of time and energy calculating a large number of nodes in [15], it is necessary to select a small number of interesting nodes to represent and predict the overall behavior of the propagation model.

Therefore, the work-flow of the proposed HPMO is illustrated in Fig. 2.

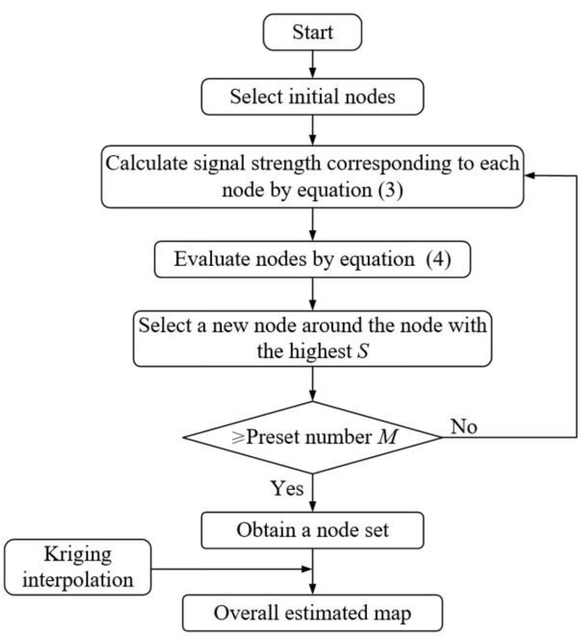

Fig. 2. Flow-chart of HPMO.

In the design process, from two initial nodes located on the diagonal of the two-dimensional space, their corresponding signal strength value are calculated by equation (3), a new node will be generated around the node with the highest ranked score S according to equation (4).

If the total number of the nodes has not yet been equal to the preset value M, a call is made to the model calculation and sequential design routine, which tends to select a new node to be evaluated, and the algorithm starts all over again. Finally, the EM signal strength distribution in the two-dimensional region is reconstructed according to the selected node and its corresponding output value.

III. NUMERICAL RESULTS

In this paper, all the simulation experiments are performed on a standard laptop with 1.6GHz CPU and 8GB of RAM.

A. Definition of indoor reference scenario

In order to gain insight into the proposed model, the considered environment in this paper is an empty indoor environment with a very complex topology and form, including the size and shape of different rooms and corridors as shown in Fig. 3.

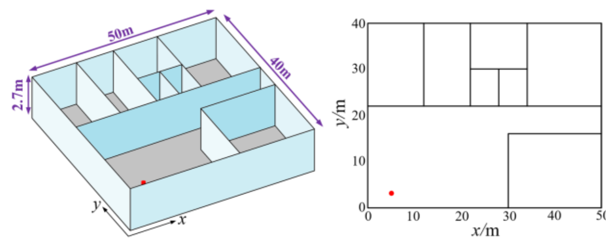

(a) (b)

Fig. 3. Schematic view (a) and top view (b) of the indoor structure and transmitter location identification.

The dot in Fig. 3 corresponds to the transmitter antenna [dipole], which is located at coordinates (x = 5 m, y = 3 m, z = 0.2 m). Specific simulation parameters are defined in Table 1.

Table 1: Simulation parameters

Parameters	Value
Frequency	2.4GHz
Transmitter power	15dB(m)
Wall permittivity	5.3
Observation plane height	0.8m
Observation range(x)	[0m,50m]
Observation range(y)	[-5m,45m]

B. Uniform meshing

During the modeling process, in order to get better resolution, the uniform mesh size must be controlled below half the wavelength, which is due to Nyquist theory. As shown in Fig. 4 [mesh size of $\lambda/2$, total nodes of 6.4×10^5], the ray tracing algorithm [15] calculates each node to obtain a signal strength distribution map of the entire observation plane.

In this indoor structure example, the grid size is closely related to the calculation time, as shown in Fig. 5. The amount of computation for the exact solution of the model tends to increase at an exponential rate with the problem size.

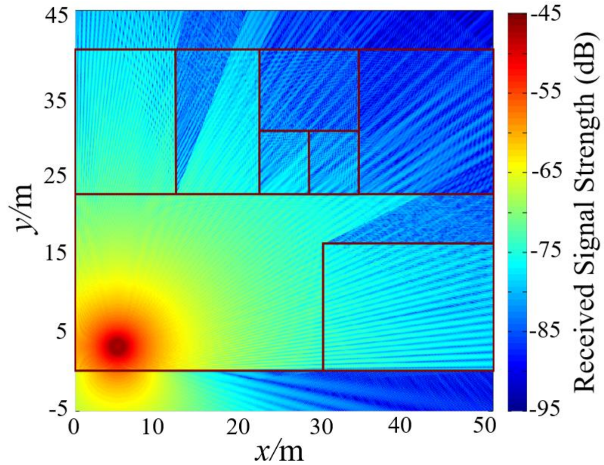

Fig. 4. EM signal strength propagation map obtained by modified Motley-Keenan model based on uniform meshing.

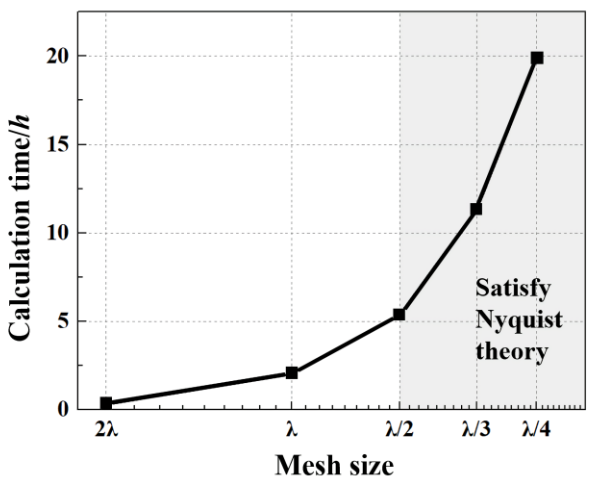

Fig. 5. The relation curve of mesh size and calculation time under uniform meshing.

C. Adaptive meshing used LOLA-Voronoi

In the study of electromagnetic field coverage in space, too fine mesh generation is not necessary. For the purpose of algorithm optimization and cost saving, the probes can be placed at interesting and representative positions, and then the signal strength in the entire 2D research area can be estimated by ordinary Kriging interpolation.

To illustrate how LOLA-Voronoi identifies nonlinear regions while still maintaining proper domain coverage, the node distributions have been obtained using the adaptive meshing strategy and random meshing respectively when the number of $M = 200$ [Fig. 6 (a), Fig. 7 (a)], and $M = 500$ [Fig. 6 (c), Fig. 7 (c)] nodes are used. Their corresponding prediction results are shown in Figs. 6 (b), (d) and Figs. 7 (b), (d).

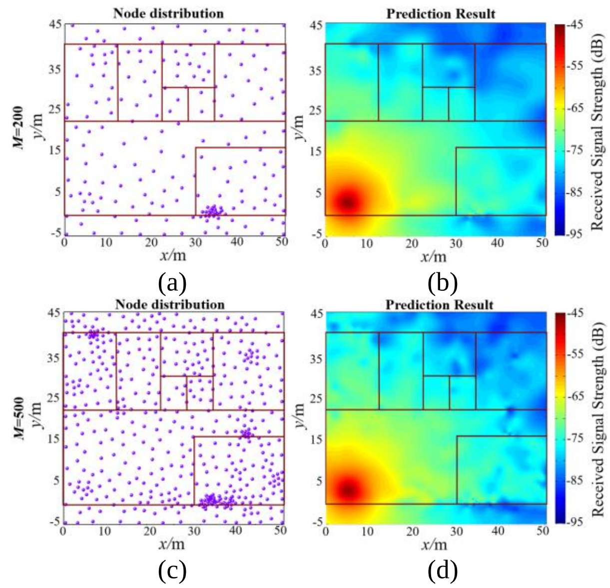

Fig. 6. The distribution of nodes by the LOLA-Voronoi adaptive meshing and the corresponding prediction map when (a), (b) M=200, (c), (d) M=500.

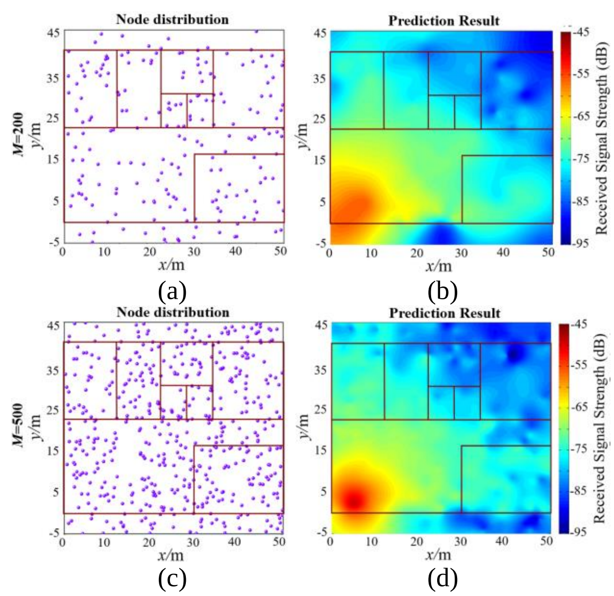

Fig. 7. The distribution of nodes by the random meshing and the corresponding prediction map when (a), (b) M=200, (c), (d) M=500.

As shown in Fig. 6, as the number of nodes increases, the intensive subdivision always occurs near the wall where the signal strength value is mutated, and under-meshed is also avoided in other areas. Because

LOLA-Voronoi is always able to capture the details of the changes in the field, and can adaptively identify the location of interest while maintaining proper coverage. Random meshing is selected for comparison, which usually lead to chaotic distribution of nodes and even under-meshed of some regions [Fig. 7].

For the intuitiveness and completeness of the conclusion, the HPMO based on LOLA-Voronoi adaptive meshing is further verified by the prediction error versus the number of nodes [Fig. 8, $10 \le M \le 1000$].

The prediction precision could be supported by defining the relative error (ξ):

$$\xi = \frac{\left\| \mathbf{s} - \hat{\mathbf{s}} \right\|_2}{\left\| \mathbf{s} \right\|_2}, \tag{9}$$

where $\mathbf{s}$ is the original data [Fig. 4] obtained by fine and uniform mesh, and $\hat{\mathbf{s}}$ is the estimated data based on the several meshing nodes. In this paper, all the prediction errors are obtained by taking the average of the relative errors of equation (9) after 50 times measurement.

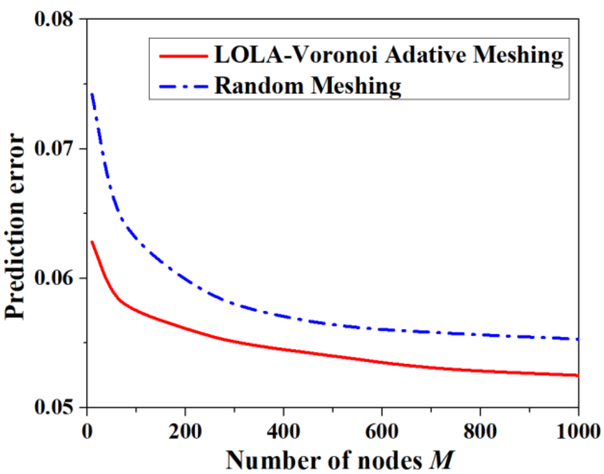

Fig. 8. *Performance Analysis*—Comparison of prediction error between LOLA-Voronoi adaptive meshing and random meshing.

In Fig. 8, LOLA-Voronoi adaptive meshing yields a certain improvement in the accuracy compared with random meshing. It is worth noticing that the fewer nodes makes the adaptive meshing more efficient than the random meshing, so as expected, the adaptive meshing strategy greatly accelerates the prediction of indoor propagation and keeps low prediction error by placing nodes in more important and interest positions.

In order to further prove the accuracy of the proposed HPMO, Table 2 lists the RMSE (Root Mean Square Error) of indoor propagation models based on the benchmark simulation data of commercial software Altair Winprop in the same reference scenario.

Table 2: RMSE of indoor propagation models

Models	RMSE(dB)
Log-distance	7.18
ITU-R [8]	8.46
Multi-wall [9],[11]	4.74
Modified Motley-Keenan [14-15]	4.65
HPMO (0.16% of total nodes)	4.69

It can be concluded from Table 2 that the HPMO proposed in this paper only needs 0.16% of the total number of nodes in the modified Motley-Keenan [14-15] model to reconstruct a result with the RMSE value of 4.69dB. It can be seen that even if the computing resources required by the original algorithm are reduced, it can still obtain sufficient prediction accuracy.

IV. CONCLUSION

In this paper, an innovative strategy for efficiently indoor propagation prediction has been proposed. In order to reduce the cost of the model program, the traditional dense uniform mesh method is replaced by an adaptive mesh method based on the output value. Accurately approximate the actual model based on a small number of interesting data points that are densely distributed in the nonlinear region and ensure that other regions are not under-meshed. Subsequently, the results from a representative set of numerical experiments have been reported and discussed to analyze the advantages of the proposed model in terms of accuracy and efficiency. The model obtained satisfactory results in the high-efficient modeling of indoor scene, and also provided an important insight into the position of measuring equipment in actual experimental measurement.

ACKNOWLEDGMENT

This work is supported by the National Key Research and Development Program of China (under Grant No. 2017YFB0503500) and the National Natural Science Foundation of China (under Grant No. 61571232).

The authors wish to thank Professor Salaheddin Hosseinzadeh for sharing the indoor radio propagation code online.

REFERENCES

[1] A. Achroufene, Y. Amirat, and A. Chibani, "RSS-based indoor localization using belief function theory," *IEEE Transactions on Automation Science and Engineering*, vol. 16, no. 3, pp. 1163-1180, July 2019.

[2] S. Sun, Y. Li, W. S. T. Rowe, et al., "Practical evaluation of a crowdsourcing indoor localization system using hidden Markov models," *IEEE Sensors Journal*, vol. 19, no. 20, pp. 9332-9340, Oct. 2019.

[3] S. Y. Lim, Z. Yun, and M. F. Iskander, "Radio

propagation modeling: A unified view of the ray-tracing image method across emerging indoor and outdoor environments," *The World of Applied Electromagnetics*, 2018.

[4] H. Y. Chen and S. H. Wen, "Evaluation of E-field distribution and human exposure for a LTE femtocell in an office," *Applied Computational Electromagnetics Society Journal (ACES)*, vol. 31, no. 4, pp. 455-467, Apr. 2016.

[5] J. Sosa, S. Coss, A. RodríGuez, et al., "Indoor 2.4GHz microwave propagation study using 3D FDTD approach," *Electronics Letters*, vol. 47, pp. 1308-1309, 2011.

[6] Z. Gu and Z. Jiang, *A Modified UTD Model for Indoor Propagation Prediction*. 2005.

[7] S. A. Mitilineos, S. C. Panagiotou, P. K. Varlamos, et al., "Indoor environments propagation simulation using a hybrid MoM and UTD electromagnetic method," *Annales des Telecommunications*, vol. 60, no. 9, pp. 1231-1243, 2005.

[8] "Propagation data and prediction methods for the planning of indoor radio communication systems and the radio local area networks in the frequency range 900 mhz to 100 ghz," *Recommendation ITU-R P.1238-8*, 2015.

[9] A. J. Motley and J. M. Keenan, "Radio coverage in buildings," *British Telecom Tech. J.*, vol. 8, no. 1, pp. 19-24, 1990.

[10] M. Hatay, "Empirical formula for propagation loss in land mobile radio services," *IEEE Transactions on Vehicular Technology*, vol. 29, no. 3, pp. 317-325, 1980.

[11] COST Action 231: Digital Mobile Radio Towards Future Generation Systems: Final Report, 1999.

[12] N. Iqbal, J. Luo, R. Müller, et al., "Multipath cluster fading statistics and modeling in millimeter-wave radio channels," *IEEE Transactions on Antennas and Propagation*, vol. 67, no. 4, pp. 2622-2632, Apr. 2019.

[13] R. Adeogun, T. Pedersen, C. Gustafson, et al., "Polarimetric wireless indoor channel modeling based on propagation graph," *IEEE Transactions on Antennas and Propagation*, vol. 67, no. 10, pp. 6585-6595, Oct. 2019.

[14] S. Hosseinzadeh, H. Larijani, K. Curtis, et al., "Empirical propagation performance evaluation of LoRa for indoor environment," *IEEE International Conference on Industrial Informatics*, 2017.

[15] S. Hosseinzadeh, "3D ray tracing for indoor radio propagation." (https: //www. mathworks.com/ matlabcentral/fileexchange/64695-3d-ray-tracing-for-indoor-radio-propagation) MATLAB Central File Exchange. Retrieved November 8, 2019.

[16] V. Moghtadaiee, S. A. Ghorashi, and M. Ghavami. "New reconstructed database for cost reduction in indoor fingerprinting localization," *IEEE Access*, vol. 7, pp. 104462-104477, 2019.

[17] B. Z. Li, M. Salucci, P. Rocca, J. Y. Yao, et al., "Total-variation compressive sensing based on hybrid sequential experimental design for field reconstruction," *Applied Computational Electromagnetics Society (ACES) Symposium*, Nanjing, China, Aug. 2019.

[18] K. Crombecq, D. Gorissen, D. Deschrijver, and T. Dhaene, "A novel hybrid sequential design strategy for global surrogate modeling of computer experiments," *SIAM Journal on Scientific Computing*, vol. 33, no. 4, pp. 1948-1974, Jan. 2011.

[19] "Effects of building materials and structures on radiowave propagation above about 100 MHz," *ITU-R P.2040-1*, 2015.

Junyi Yao was born in Jiangsu Province, China, in 1995. She received the B.S. degree from Nanjing Normal University (NJNU), Nanjing, in School of Physics and Technology in 2017. She is currently pursuing the M.S. degree with the School of Physics and Technology, NJNU.

Her current research interests include numerical calculation of EM field and reconstruction algorithm.

Wanchun Tang (M'04) was born in China in 1967. He received the B.S. degree from Tsinghua University, Beijing, China, in 1990, the M.S. degree from the Nanjing University of Science and Technology (NJUST), Nanjing, China, in 1995, and the Ph.D. degree from the City University of Hong Kong, Hong Kong, in 2003, all in Electrical Engineering.

He was a Full Professor with the Department of Communication Engineering, NJUST, and is currently a Specially Invited Full Professor with the Jiangsu Key Laboratory on Optoelectronic Technology, School of Physics and Technology, Nanjing Normal University, Nanjing. He has authored or coauthored over 100 journal and conference papers. His current research interests include modeling and optimization of RFIC, antennas, signal integrity, and power integrity design in package.